DO Note 6091-CONF

Search for Associated Higgs Boson Production with Like-Sign Leptons in $p\bar{p}$ Collisions at $\sqrt{s} = 1.96$ TeV

The DØ Collaboration
URL http://www-d0.fnal.gov
(Dated: July 20, 2010)

We search for associated Higgs boson production in the process $p\bar{p} \to V(W/Z)H \to \ell^{\pm}\ell'^{\pm} + X$ in ee, $e\mu$, and $\mu\mu$ final states. The search is based on data taken at the Fermilab Tevatron at $\sqrt{s} = 1.96$ TeV corresponding to 5.4 fb^{-1}. We require two like-sign isolated leptons (electrons or muons) with $p_T > 15$ GeV plus additional selection cuts. No significant excess is observed, and we set 95% C.L. observed (expected) upper limits on σ(VH)×Br(VH→ $\ell^{\pm}\ell^{\pm}$ + X) as ratios to the Standard Model cross section between 18.1 (13.2) and 5.9 (6.8) for Higgs masses from 115 to 200 GeV.

Preliminary Results for Summer 2010 Conferences

I. INTRODUCTION

In the standard model, the Higgs boson predominantly decays to a WW^* pair for Higgs boson masses above 135 GeV and also to a $\tau\tau$ pair for lower masses [1], both of which decay to leptonic final states involving neutrinos with large branching fractions. In fermiophobic Higgs models, the branching ratio $Br(H \rightarrow WW^*)$ may be close to 100% for Higgs masses down to ∼100 GeV [2]. Consequently the associated production of Higgs boson, $p\bar{p} \rightarrow V(W/Z)H \rightarrow \ell^{\pm}\,\ell^{\pm} + X$ which has an easily-detected experimental signature, provides a search mechanism for both standard model and fermiophobic Higgs. As opposed to the direct Higgs production, $p\bar{p} \rightarrow H \rightarrow WW^*$, in associated production there are two leptons of the same electrical charge. This like-charge signature is used to perform a search which is orthogonal and complementary to the inclusive search for the dilepton signal which considers mainly the direct production and requires opposite-sign leptons.

The requirement of like-charge suppresses most of the standard model processes which have final states with oppositely charged leptons, such as ($p\bar{p} \rightarrow Z/\gamma^*$, $p\bar{p} \rightarrow WW$, and $p\bar{p} \rightarrow t\bar{t}$. The physics sources to the like-charge leptons arise from $p\bar{p} \rightarrow WZ \rightarrow \ell\nu\ell\ell$ and $p\bar{p} \rightarrow ZZ \rightarrow \ell\ell\ell\ell$ processes which have small production cross section. The non-resonant triple vector boson production (VVV, $V = W, Z$) and the production of $t\bar{t} + V$ are negligibly small.

There are also two instrumental backgrounds. The first, "charge flips", originates from the misreconstruction of the charge of one of the leptons. For the same lepton flavor channels (ee and $\mu\mu$) this background has the underlying physics of the Drell-Yan process, $p\bar{p} \rightarrow Z/\gamma^* \rightarrow \ell^+\ell^-$. When the two leptons are of different flavor, this background is negligible. The second instrumental background is jets from QCD-produced multijet events. The jets may be identified as isolated leptons with high transverse momenta with respect to the beam axis (p_T).

The W production with associated jets is a semi-instrumental background to the dilepton selection, where one of the lepton candidates is a jet. The kinematics of the W+jets and the presence of a neutrino makes this background difficult to discriminate in contrast to other instrumental backgrounds.

As there may be multiple neutrinos in the final state, complete reconstruction of the Higgs mass in the candidate events is not feasible. A potential Higgs boson signal would appear as an excess in the number of observed events with two like-sign leptons and certain kinematic properties resulting from the rest of the event and the missing energy from the neutrinos. A multivariate technique is employed to form a single discriminant using multiple input variables to extract a maximum separation between signal and background processes. In the absence of an excess over the expected number of events from background processes, upper cross section limits are set. These limits vary with the Higgs mass in the range of 115 to 200 GeV.

Previously DØ published a $WH \rightarrow WWW^* \rightarrow \ell^{\pm}\ell^{\pm} + X$ search based on approximately 0.4 fb^{-1} of data [3]. An update [4] based on about 1 fb^{-1} of data was presented in the summer of 2007. Additional dataset was analyzed in winter 2009 with a preliminary result based on 2.5 fb^{-1} combined with the previous 1 fb^{-1} result [5]. This note describes the unified inclusive like-sign leptons search for the Tevatron data up to the summer 2009 which includes all the dataset covered by the previous analyzes. The dataset corresponds to 5.4 fb^{-1} of integrated luminosity of reconstructed good quality data.

II. THE DØ DETECTOR

The DØ detector has a central-tracking system, calorimeters, and a muon spectrometer [6]. The central tracking system includes a silicon microstrip tracker (SMT) and a central fiber tracker (CFT) embedded in 2 T solenoidal magnetic field, and provides tracking in the pseudorapidity range of $|\eta| < 3$. The uranium/liquid argon calorimeter consists of a central section (CC) covering pseudorapidities η up to ≈ 1.1, and two end calorimeters (EC) that extend coverage to $\eta \approx 4.2$. The muon detection system surrounds the calorimeters and allows for detection of muons at pseudorapidities $|\eta| < 2$. It is a toroidal spectrometer and provides a second measurement of p_T and electrical charge. Timing information is recorded in the muon system and is used to veto activity from cosmic rays. Luminosity is measured from the $p\bar{p}$ inelastic collision rate using plastic scintillator arrays.

III. DATA AND MONTE CARLO SAMPLES

This analysis uses data collected by the DØ experiment during two data taking periods: from April 2002 to February 2006 referred to as "Run IIa" and from June 2006 to June 2009 referred to as "Run IIb". The data samples corresponds to integrated luminosities of 1.1 fb^{-1} and 4.3 fb^{-1} for Run IIa and Run IIb respectively.

The signal and the physics background processes are modeled by the Monte Carlo (MC) simulation. The MC event samples are generated with PYTHIA version 6.323 [7] using CTEQ6L1 parton density functions and with a detailed GEANT 3 based [8] simulation of the DØ detector. The signal cross section is calculated at NNLO using HDECAY [9]

and the Higgs boson decay branching ratios are taken from PYTHIA. The diboson production cross sections are taken to be the NLO values recommended by the Tevatron New Phenomena and Higgs Working Group [10]. For the W+jets processes including the Heavy Flavor emission, matrix element based ALPGEN [11] event generator is used with an interface to PYTHIA for hadronization.

The MC samples are normalized to theoretical cross sections multiplied by the integrated luminosity of the data samples, with an additional corrections to account for the event reconstruction and selection efficiencies. These factors are obtained by normalizing the number of unlike charged dilepton events in the $Z \rightarrow \ell\ell$ peak. The Z/$\gamma*$ cross section is calculated with CTEQ6.1M PDFs using the NNLO to LO K-factor according to [12]. This procedure is explained in Section V.

For the instrumental backgrounds, charge flip and multijet, no attempt is made to estimate their contributions from known cross sections and detector simulation, as such a calculation is not expected to be reliable. Instead, these rates are measured in the data. In that case, MC samples are used only for additional information about the shape of the backgrounds.

IV. EVENT SELECTION

The analysis starts with the selection of events that have at least two lepton candidates, which can be either electrons or muons. There is no explicit trigger requirement applied, however, most of the events are collected by the single lepton or double lepton triggers.

For electrons, we require a cluster of electromagnetic (EM) energy in the central calorimeter region ($|\eta| < 1.1$) with $p_T > 15$ GeV, matched to a track in the central tracker. The electron energy is reconstructed in a cone of radius, $\mathcal{R}$ = 0.2, where $\mathcal{R} = \sqrt{(\Delta\eta)^2 + (\Delta\phi)^2}$ and ϕ is the azimuthal angle. The electromagnetic energy fraction is required to be greater than 0.9, and the isolation fraction less than 0.2, where the isolation fraction is defined as the ratio of the calorimeter deposition in the annulus between radii, $0.2 < \mathcal{R} < 0.4$, to the electron energy. These electrons are called "loose" and are used to estimate the multijet background. The signal search proceeds with electrons that further pass a cut on calorimeter energy over track momentum, $0.5 < E/p < 3$, and also pass a cut on an eight variable likelihood discriminant that selects isolated prompt electrons. These are called "tight" electrons.

For muons, we require muon spectrometer activity that passes cosmic ray veto timing cuts and which matches a $p_T > 15$ GeV track in the central tracker. The reconstructed pseudorapidity must satisfy $|\eta| < 1.8$ and to reduce charge flip backgrounds, the constraint $p_T < 200$ GeV is applied. Requiring that the track emanates from the primary interaction point improves the purity of this "loose" muon sample, as does the requirement that the track also does not match an EM cluster and be separated from identified jets by more than $\Delta\mathcal{R} = 0.1$. The sum of energy in the calorimeter within a hollow cone $0.1 < \mathcal{R} < 0.4$ around the track $\sum_{0.1<\mathcal{R}<0.4} E_T^{cell}$ must be less than 2.5 GeV, and the sum of p_T of all tracks in the cone $\mathcal{R} < 0.5$ around the muon's track $\sum_{\mathcal{R}<0.5} p_T^{trk}$ also must be less than 2.5 GeV.

An additional set of track quality cuts, aimed at further reducing the charge flip background, are applied to the tight lepton samples. These include requirements on the maximum distance in the direction of the beam axis between the lepton tracks and the vertex (1 cm), a maximum distance of closest approach to the primary vertex $dca < 0.01$ cm and its significance $|dca/\sigma(dca)| < 5$, $\chi^2/NDF < 5$ for the lepton track fit, and a minimum number of SMT and CFT measurements of 1 and 12 respectively.

The efficiency of the lepton selection (trigger, lepton quality and track quality cuts) in MC samples are corrected by the data-to-MC scale factors explained in Section V.

Further kinematic cuts are applied to reduce instrumental backgrounds and to select a well understood region of phase space for the analysis. Both leptons are required to come from the primary vertex and have the same charge. An upper cut is placed on the track momentum, $p_T < 200$ GeV, and the dilepton invariant mass has to be 15 GeV $< m_{\ell\ell} <$ 250 GeV. To keep the analysis sample orthogonal to the inclusive $H \rightarrow WW^*$ search [13], events are rejected if the leading two leptons, selected under the same requirements applied in the inclusive analysis, are oppositely charged.

Control regions are used for estimating the charge flip contribution in ee channel and multijet contributions in ee and $\mu\mu$ channels in like-sign data, as explained in Section V. The kinematic regions are defined by the dilepton invariant mass, $m_{\ell\ell}$, and the azimuthal separation between the two leptons, $\Delta\phi_{\ell\ell}$, to enhance the fraction of charge flip or multijet events and minimize the physics content. The signal contribution is assumed negligible. The charge flip control region for ee channel is,

$$85 \text{ GeV} < m_{\ell\ell} < 100 \text{ GeV and } \Delta\phi_{\ell\ell} > 2.8$$

The multijet control region for ee and $\mu\mu$ is,

$$30 \text{ GeV} < m_{\ell\ell} < 50 \text{ GeV and } \Delta\phi_{\ell\ell} > 2.5$$

These control regions are removed from the analysis, and the remaining events are referred to be in "signal search region".

The final stage of the selection uses a discriminant variable obtained from multivariate analysis. The details can be found in Section VII.

V. BACKGROUNDS

The estimation of the four types of background processes, physics (diboson), W+jet, charge flip and multijet, are explained in this section.

A. Physics background

The physics background (true like-sign isolated high p_T leptons) is primarily from $p\bar{p} \to WZ \to \ \ell^{\pm}\nu\ell^{\pm}\ell^{\mp}$, where the two lepton candidates that form the like-sign pair have the leading p_T, or where the third lepton is unidentified. The process, $p\bar{p} \to ZZ \to \ \ell^{\pm}\ell^{\mp}\ell^{\pm}\ell^{\mp}$, has a smaller cross section but two possibilities for a like-sign pair. This background is estimated from the known cross sections,

$$\begin{aligned} \sigma(p\bar{p} \to WZ) &= 3.45 \pm 0.24\ pb \\ \sigma(p\bar{p} \to ZZ) &= 1.37 \pm 0.10\ pb \end{aligned}$$

and the branching ratios of Z and W boson decays.

The MC generated events are normalized to the theoretical cross section multiplied by the integrated luminosity. Scale factors are applied to correct for the known differences in the particle level kinematics and object reconstruction and identification efficiencies between the data and the simulation. An additional normalization factor is obtained from unlike-sign events by scaling the sum of MC predictions to match the data under the Z mass peak to account for the residual difference in the yield due to the additional lepton and track quality requirements.

Having no explicit trigger requirement, the events may not have been triggered by the dileptons, but by other objects in the event. To emulate this effect, the ratio of the inclusive data yield to the dilepton triggered events is parameterized for different jet multiplicities [14] and applied to the simulated events. This correction is only available for dimuon events since the trigger efficiencies for high p_T electrons are known to be close to 100%.

B. W+jet background

The contribution from W production with one or more associated jets is estimated using simulated samples. The absolute normalization of the W+jet content is obtained from the MC efficiency of selecting two tight leptons with all the standard lepton ID corrections applied for all physics backgrounds as described in Section V A. The lepton fake rate in simulation may not represent that in data, and the data-MC lepton identification efficiency scale factor obtained for true leptons may not apply for fake leptons. A systematic uncertainty is assigned to the prediction of W+jet.

In $e\mu$ channel, the method to estimate the multijet contribution also accounts for W+jet where the electron candidate originates from a jet. This process is hence removed from the selected MC W+jet events.

To gain enough statistics of simulated events to model the shape of the W+jet background, the lepton identification criteria has been relaxed; the muon isolation and the electron likelihood requirements are removed.

C. Charge flip background

The charge flip background, created by the misreconstruction of the charge of one of the leptons, is mostly from the Z/γ^* process. This occurs when the track curvature is not correctly measured which may happen in particular at high p_T, or when additional hits from other charged particles and noise are present near the track. For electrons, conversion of photons from bremsstrahlung radiation is also considered as a part of the charge flip background in the like-sign sample although their charge may be correctly measured.

The contribution from the charge flips in the $\mu\mu$ selection is estimated using two measurements of the same charge. The first one is the measurement of the track charge in the central tracker, and the second measurement called the "local" muon charge as measured by the muon spectrometer. The second measurement is of much lower reliability

than the first measurement. The fraction of the charge flips is derived from the number of events where the two measurements give the same answer for both leptons (SS), agree for one lepton and disagree for another one (OS), or disagree for both leptons (OO). The expected number of events in these three categories, N_{SS}, N_{OS} and N_{OO}, depends on the fraction of the $\mu\mu$ sample that are charge flip events, $N_{flip}/(N_{true}+N_{flip})$, and on the efficiency of the local charge measurement, ε_{loc}.

$$\begin{aligned} N_{SS} &= P_{SS}^{true}(\varepsilon_{loc})N_{true} + P_{SS}^{flip}(\varepsilon_{loc})N_{flip} \\ N_{OS} &= P_{OS}^{true}(\varepsilon_{loc})N_{true} + P_{OS}^{flip}(\varepsilon_{loc})N_{flip} \\ N_{OO} &= P_{OO}^{true}(\varepsilon_{loc})N_{true} + P_{OO}^{flip}(\varepsilon_{loc})N_{flip}, \end{aligned} \quad (1)$$

The efficiency is measured using unlike-sign data in the $Z \rightarrow \mu\mu$ resonance and parameterized as a function of $1/p_T$. Once the efficiency has been measured, the charge flip fraction can be determined from the number of events in the 3 categories observed in the data. The method predicts ∼half of the like-sign events to be charge flip after the track quality based selection, which translates to a charge mismeasurement rate of approximately 10^{-4} in the dilepton sample dominated by $Z \rightarrow \mu\mu$ with muon $p_T \sim 45$ GeV.

The contribution of the charge flips in ee events is obtained by multiplying the charge flip rate (the ratio of like-sign to either-sign dielectron events) by the number of either-sign dielectron events in data. The charge flip rate and the product with the number of either-sign dielectron events in the data are parameterized with the p_T of that lepton which has the largest p_T in the event. The charge flip rate is first derived using MC $Z \rightarrow e^+e^-$ events over the full range of p_T values used in the analysis. It is then scaled by the ratio of rates in data *vs.* MC in the control region defined in Section IV. The known contaminations from other physics sources in the control region is subtracted from data. The charge flip rate measured in data is typically 4×10^{-4} after all the cut based selection.

The fraction of charge flips in the $e\mu$ channel is negligible as the $Z/\gamma* \rightarrow \tau^+\tau^- \rightarrow \ell^+\ell^-$ is suppressed by the branching fraction of the tau into electrons and muons. In addition, leptons from τ decays have lower p_T, so fewer of them pass the 15 GeV p_T cut, and those that do have a low charge flip fraction because of their low momentum. An upper limit on the contribution from the Drell-Yan production of τ pairs may be obtained from the product of the average electron and muon charge flip rates referenced to the number of either-sign events with the number of unlike-sign $e\mu$ events observed. This is about one event after all the track quality requirements, and this estimate does not account for the different p_T spectrum from τ events.

The kinematic distributions of the charge flip events are modeled by unlike-sign data since the charge flip is expected to originate mainly from $Z \rightarrow \ell\ell$ process which also dominates unlike-sign data. Corrections are applied to the lepton kinematics to account for the effect of the charge mismeasurement. The charge flip rate of a single isolated lepton is first measured using MC samples by identifying the charge flip leptons from the generator level information. The rate per lepton (as opposed to rate per event used for charge flip estimation in ee) is parameterized as a function of p_T and detector η, and applied to the unlike-sign data as an event weight. The rate for a given event is decided randomly over the ratio of two charge flip rates. For dimuon events, an oversmearing to the track momentum is obtained from the charge flip MC events and applied to the lepton which is chosen to have flipped.

D. Multijet background

The multijet background, in the case of jets misidentified as muons, contains muons from semileptonic heavy flavor, punch-through hadrons misidentified as muons, and muons from pion or kaon decays in flight. In the case of jets misidentified as electrons, the multijet background contains electrons from semileptonic heavy flavor decays, from hadrons misidentified as electrons, and from γ conversions.

The fraction of like-sign events due to multijet may be calculated from the fraction of loose dilepton events without tight leptons (N_0) and with exactly one tight lepton (N_1). Assuming that these samples consist mostly of fake leptons which have probability ε_Q to be identified as tight with a correlation of ε_Q between the two leptons being ρ,

$$N_0 = (1-\varepsilon)(1-\varepsilon[1-\rho]) \quad (2)$$

$$N_1 = 2\varepsilon(1-\varepsilon)[1-\rho] \quad (3)$$

Consequently, $N_{QCD} = \varepsilon^2[1-\rho] + \rho\varepsilon$. For each channel, ee and $\mu\mu$, the equation is solved for the values of ε and ρ using events in a multijet control region defined in Section IV where the multijet content is high. The small contribution from dibosons predicted from the simulated samples is subtracted from the N_0 and N_1 counts. The contamination from the W+jet and charge flip is less precisely known, hence treated as the systematic uncertainty of

TABLE I: The number of predicted and observed events at preselection (stage0), after the track quality cuts (stage1), and at the final selection (stage2) after a cut on the multivariate discriminant. The signal event yields are based on the standard model Higgs boson production cross section and the decay branching ratio. The numbers correspond to the signal search region, excluding the two control regions used for the charge flip and multijet estimates. Statistical and systematic uncertainties have been combined.

	ee channel			$\mu\mu$ channel			$e\mu$ channel		
	stage0	stage1	stage2	stage0	stage1	stage2	stage0	stage1	stage2
$WZ \to \ell\nu\ell\ell$	4.5 ± 0.3	3.9 ± 0.3	3.5 ± 0.3	7.9 ± 0.6	6.8 ± 0.5	4.3 ± 0.3	12.9 ± 0.9	11.1 ± 0.8	9.3 ± 0.7
$ZZ \to \ell\ell\ell\ell$	0.82 ± 0.05	0.69 ± 0.05	0.21 ± 0.01	1.18 ± 0.08	1.03 ± 0.08	0.62 ± 0.04	2.11 ± 0.15	1.83 ± 0.13	1.38 ± 0.1
W+jet	9.0 ± 1.8	8.2 ± 1.6	6.4 ± 1.3	4.3 ± 0.8	3.4 ± 0.7	2.1 ± 0.4	2.9 ± 0.5	2.1 ± 0.4	1.25 ± 0.04
multijet	29.1 ± 9.2	19.2 ± 6.7	1.3 ± 0.5	24.5 ± 7.7	18.2 ± 5.9	5.5 ± 1.8	134.5 ± 28.6	90.6 ± 20	12.2 ± 2.6
charge flip	73.7 ± 8.7	18.1 ± 4.9	0.7 ± 0.1	166.0 ± 21.3	16.8 ± 9.4	4.6 ± 2.7	0.0 ± 0.0	0.0 ± 0.0	0.0 ± 0.0
total	117.1 ± 12.8	50 ± 8.6	12 ± 1.5	204.0 ± 22.7	46.2 ± 11.1	17.2 ± 3.3	152.4 ± 28.6	105.7 ± 20	24.12 ± 2.6
data	117	39	13	167	31	18	113	82	20
$VH(120)$	0.36 ± 0.03	0.28 ± 0.02	0.24 ± 0.02	0.55 ± 0.04	0.43 ± 0.03	0.26 ± 0.01	0.95 ± 0.08	0.75 ± 0.06	0.59 ± 0.05
$VH(160)$	0.51 ± 0.04	0.44 ± 0.04	0.39 ± 0.03	0.68 ± 0.05	0.6 ± 0.04	0.56 ± 0.04	1.19 ± 0.1	1.02 ± 0.09	0.93 ± 0.08
$VH(200)$	0.21 ± 0.02	0.18 ± 0.02	0.17 ± 0.01	0.28 ± 0.02	0.25 ± 0.01	0.21 ± 0.01	0.52 ± 0.04	0.45 ± 0.04	0.41 ± 0.03

the two parameters. Once N_{QCD} is determined in the control region, it is scaled using the number of events without tight leptons in the signal search region.

The number of multijet events in the $e\mu$ sample is estimated using the sample with a tight muon and any electron. The distribution of the eight variable likelihood discriminant for EM clusters is fitted using templates for true and fake electrons. The true electron likelihood distribution is taken from events in the unlike sign data at the Z resonance. The likelihood distribution for jets faking electrons is taken from events in the same multijet control region in the like-sign ee data.

The shape of the kinematic distributions from multijet is modeled by events from like-sign data which do not pass the tight lepton quality. The lepton quality requirements are inverted for both leptons in ee and $\mu\mu$ channels. Only one lepton quality is inverted and the other is kept tight for $e\mu$ channel since a significant fraction of events are expected to be W+jet.

VI. EVENT SAMPLE COMPOSITION

The number of predicted and observed events after all selections in the total integrated luminosity of 5.4 fb^{-1} is summarized in Table I. In all channels, the observed number of events is in agreement with the sum of predicted background. Some selected kinematic distributions are shown in Figure 1 before and after the track quality requirements. They show that the shape of the background distributions is well modeled by the sample described in Section V and that the sample composition is correctly predicted.

VII. MULTIVARIATE METHOD

After selection of events with high p_T same-charge lepton pairs, and understanding the background contributions as described above, we construct a variable to separate the signal from the major backgrounds using a multivariate technique. This variable is used to derive the statistical interpretation of the data for the presence of the Higgs boson signal (Section VIII). The final discriminant is built in two steps: the first step is optimized to reject as much instrumental background as possible, and the second step is dedicated to separating the diboson background from the Higgs signal.

The `TMVA` package [15] has been used to construct, test, and implement the discriminants. Amongst several available algorithms, Boosted Decision Tree with Gradient boost (BDTG) has been found to provide excellent signal and background separation, maximum use of variable correlations and robustness against low statistics which is particularly beneficial to the like-sign search.

The training samples are selected in the same way as those used for the analysis as explained in Section V. Approximately half of the statistics is used for the training, and the other half is used for testing and to obtain the results. The overtraining is checked by comparing the output distributions of the training and testing samples which are randomly picked from the combined samples.

The variables considered for the training are:

- Dilepton angular separation: $\Delta\eta$, $\Delta\phi$, ΔR
- Kinematics of all leptons in the event:
  Lepton multiplicity (N_{Leps}), p_T of the all-lepton system (p_{TLeps}), scalar sum of lepton p_T (SET_{Leps})
- Kinematics of all jets in the event:
  Jet multiplicity (N_{Jets}), p_T of the all-jet system (HT), scalar sum of jet p_T (SHT)
- Kinematics of all the objects (leptons and jets) in the event:
  Object multiplicity (N_{Objs}), p_T of the all-object system (p_{TObjs}), scalar sum of object p_T (SET_{Objs})
- Missing E_T:
  Standard MET, special $specMET$, perpendicular $perpMET$
- Dilepton - missing E_T relation:
  minimum/maximum transverse mass ($M_T(\ell, MET)^{min/max}$), maximum/minimum azimuthal separation ($\Delta\phi(\ell, MET)^{min/max}$)
- Invariant mass between any opposite-sign lepton pair with value closest to Z mass (default = 0)

The variables $perpMET$ and $specMET$ are designed to provide information about the missing E_T that is not due to mismeasurement of object momenta. To derive $perpMET$, we start from the object that has the smallest angular separation to the axis of the missing E_T in the transverse plane. Then the component of the missing E_T that is perpendicular to the object momentum is used. For $specMET$, all leptons and jets are considered and the missing E_T is recalculated only when the azimuthal separation is less than pi/2. For $perpMET$, only the like-sign dileptons are considered, and for the $e\mu$ selection the component perpendicular to the muon is always used.

Some of the variables are excluded from the training when the variables are not well modeled by the prediction or have little discrimination power on top of other variables. The variables used for each training are,
Charge flip in ee: $\Delta\eta$, N_{Leps}, p_{TLeps}, SET_{Leps}, N_{Objs}, p_{TObjs}, SET_{Objs}, MET, $M_T(\ell, MET)^{min/max}$
Charge flip in $\mu\mu$: $\Delta\eta$, $\Delta\phi$, ΔR, N_{Jets}, HT, SHT, $perpMET$
Multijet in $e\mu$: $\Delta\phi$, ΔR, p_{TLeps}, SET_{Leps}, N_{Objs}, SET_{Objs}, all missing E_T related variables
Diboson for all channels: $\Delta\eta$, $\Delta\phi$, ΔR, p_{TLeps}, HT, SHT, p_{TObjs}, SET_{Objs}, all missing E_T related variables except $specMET$

After the first step of training against instrumental backgrounds, a cut is applied on the BDT output distribution at BDT(instr) > 0.0. The cut value is chosen such that the signal efficiency is 90% or higher at a Higgs boson mass of 160 GeV. The second training against diboson background is carried out using only the events which passed this cut. To extract maximum power from the two trainings, the final discriminant is chosen to be the effective product between the two BDT outputs after the cut, shifted and renormalized to fit in the same range of -1.0 to 1.0. The results of the BDT training are shown in Figures 2.

VIII. RESULTS

In absence of an excess in the number of observed events over the standard model background, cross section upper limits have been calculated using a modified frequentist approach [17]. The systematic uncertainty of the signal and background predictions are included in the calculation, taking into account the correlation between uncertainties when present.

The systematic uncertainty for the signal and the physics background processes predicted using simulated samples arises from the precision and accuracy of the trigger and object reconstruction and identification efficiencies, and the theoretical cross section of the physics backgrounds, which amount to a total uncertainty of ∼10-12%. For W+jet, an additional 20% uncertanty is assigned for the fake lepton rate. The main source of systematic uncertainty on instrumental background is the limited statistic of the like-sign data used. Uncertainty in the parameterization of rate and possible contamination from physics sources are also included. The uncertainty in the instrumental background yields vary from ∼20% up to ∼150% depending on the channel.

The results of these calculations obtained for the 5.4 fb^{-1} of Tevatron Run II data are summarized in Table II. Figures 3 show the observed an expected cross section limits as the ratio to the standard model cross section and the log likelihood ratio (LLR) as a function of the Higgs boson mass.

TABLE II: The expected(observed) production cross section limits in terms of the ratio to the standard model cross section for individual channels and for the combination.

m_H [GeV]	ee channel		$\mu\mu$ channel		$e\mu$ channel		combined	
	expected	observed	expected	observed	expected	observed	expected	observed
115	41.3	34.5	47.7	39.6	27.3	25.9	19.8	15.9
120	37.3	29.3	36.9	48.4	22.0	22.6	16.2	16.9
125	28.7	21.4	34.0	39.4	18.5	21.2	13.4	13.2
130	24.6	18.3	26.2	31.6	15.0	12.9	10.9	9.3
135	21.4	19.3	24.3	26.3	13.5	10.9	9.6	8.1
140	18.4	12.7	21.6	24.0	12.0	10.6	8.5	6.6
145	17.9	14.5	21.5	28.1	10.6	10.0	7.8	7.6
150	17.1	14.3	20.0	26.8	10.3	9.2	7.4	7.2
155	15.8	14.6	19.8	26.5	9.5	7.2	6.8	5.9
160	15.9	15.7	20.0	24.1	10.0	7.5	7.1	6.4
165	16.8	14.2	20.1	31.0	9.8	8.5	7.0	7.2
170	17.3	18.8	22.9	29.8	9.9	9.7	7.2	8.7
175	18.4	16.6	24.1	28.6	11.2	10.8	8.0	8.0
180	19.7	22.1	26.1	28.4	12.0	11.6	8.5	9.2
185	22.7	21.4	32.5	33.7	13.6	18.8	9.9	12.1
190	26.8	24.2	38.0	46.2	15.3	20.3	11.5	14.4
195	29.0	40.2	41.4	47.9	16.1	19.9	12.0	18.2
200	31.3	33.5	44.1	49.4	17.6	25.3	13.2	18.1

IX. CONCLUSIONS

A search for the associated production of Standard Model Higgs boson, $p\bar{p} \rightarrow V(W/Z)H$, is performed with a final state with two like charge leptons, $VH \rightarrow \ell^{\pm}\ell'^{\pm} + X$, in the ee, $e\mu$ and $\mu\mu$ channels. After the final selection, 13 events in the ee channel, 20 events in the $e\mu$ channel, and 18 events in the $\mu\mu$ channel have been observed in agreement with the predicted standard model background. The observed (expected) upper limits on $\sigma(VH) \times Br(VH \rightarrow \ell^{\pm}\ell^{\pm} + X)$ for the combination of all three channels at the total integrated luminosity of 5.4 fb^{-1} are found to be between 18.1 (13.2) and 5.9 (6.8) for Higgs boson masses from 120 to 200 GeV.

Acknowledgments

We thank the staffs at Fermilab and collaborating institutions, and acknowledge support from the DOE and NSF (USA); CEA and CNRS/IN2P3 (France); FASI, Rosatom and RFBR (Russia); CAPES, CNPq, FAPERJ, FAPESP and FUNDUNESP (Brazil); DAE and DST (India); Colciencias (Colombia); CONACyT (Mexico); KRF and KOSEF (Korea); CONICET and UBACyT (Argentina); FOM (The Netherlands); PPARC (United Kingdom); MSMT (Czech Republic); CRC Program, CFI, NSERC and WestGrid Project (Canada); BMBF and DFG (Germany); SFI (Ireland); Research Corporation, Alexander von Humboldt Foundation, and the Marie Curie Program.

[1] M. Spira, in Proceedings for "Physics at Run II: Workshop on Supersymmetry / Higgs", 19-21 Nov 1998, Batavia IL U.S.A., arXiv:hep-ph/9810289 (1998).
[2] L. Brucher and R. Santos, Eur. Phys. J. C **12**, 87 (2000).
[3] The DØ collaboration, "Search for Associated Higgs Boson Production WH→WWW* → $\ell^{\pm}\nu$ $\ell'^{\pm}\nu'$+X in $p\bar{p}$ collisions at $\sqrt{s}$ =1.96 GeV", Phys. Rev. Lett. 97, 151804 (2006).
[4] The DØ Collaboration, DØ Conference Note 5485 (2007).
[5] The DØ Collaboration, DØ Conference Note 5873 (2009).
[6] V. M. Abazov *et al.*, (DØ Collaboration), Nucl. Instrum. Methods Phys. Res. A **565**, 463 (2006).
[7] T. Sjöstrand *et al.*, Comp. Phys. Comm. **135**, 238 (2001).
[8] CERN Program Library, `http://wwwasd.cern.ch/wwwasd/cernlib`.
[9] A. Djouadi *et al.*, Comp. Phys. Comm. **108**, 56 (1998).
[10] The TEVNPH Working Group (The CDF and DØ Collaborations), FERMILAB-PUB-09-060-E and `http://tevnphwg.fnal.gov`; see also J. M. Campbell and R. K. Ellis, Phys. Rev. D **60**, 113006 (1999).

[11] M. Mangano *et al.*, JHEP 0307, 001 (2003).
[12] R. Hamberg, W. L. van Neerven, and T. Matsuura, Nucl. Phys. **B359**, 343 (1991) [Erratum-ibid. **B644**, 403 (2002)].
[13] DØ Collaboration, DØ Conference Note 6082 (2010).
[14] DØ Collaboration, DØ Conference Note 6089 (2010).
[15] `http://tmva.sourceforge.net`
[16] T. Carli and B. Koblitz, Nucl. Instrum. Methods A **501**, 576 (2003).
[17] T. Junk, Nucl. Instrum. Methods A **434**, 435 (1999).
[18] DØ Collaboration, DØ Conference Note 5485 (2007).
[19] V. M. Abazov *et al.*, (DØ Collaboration), Phys. Rev. Lett. **97**, 151804 (2006).
[20] T. Aaltonen *et al.*, (The CDF Collaboration),CDF/ANAL/EXOTIC/PUBLIC/7307 (2008).

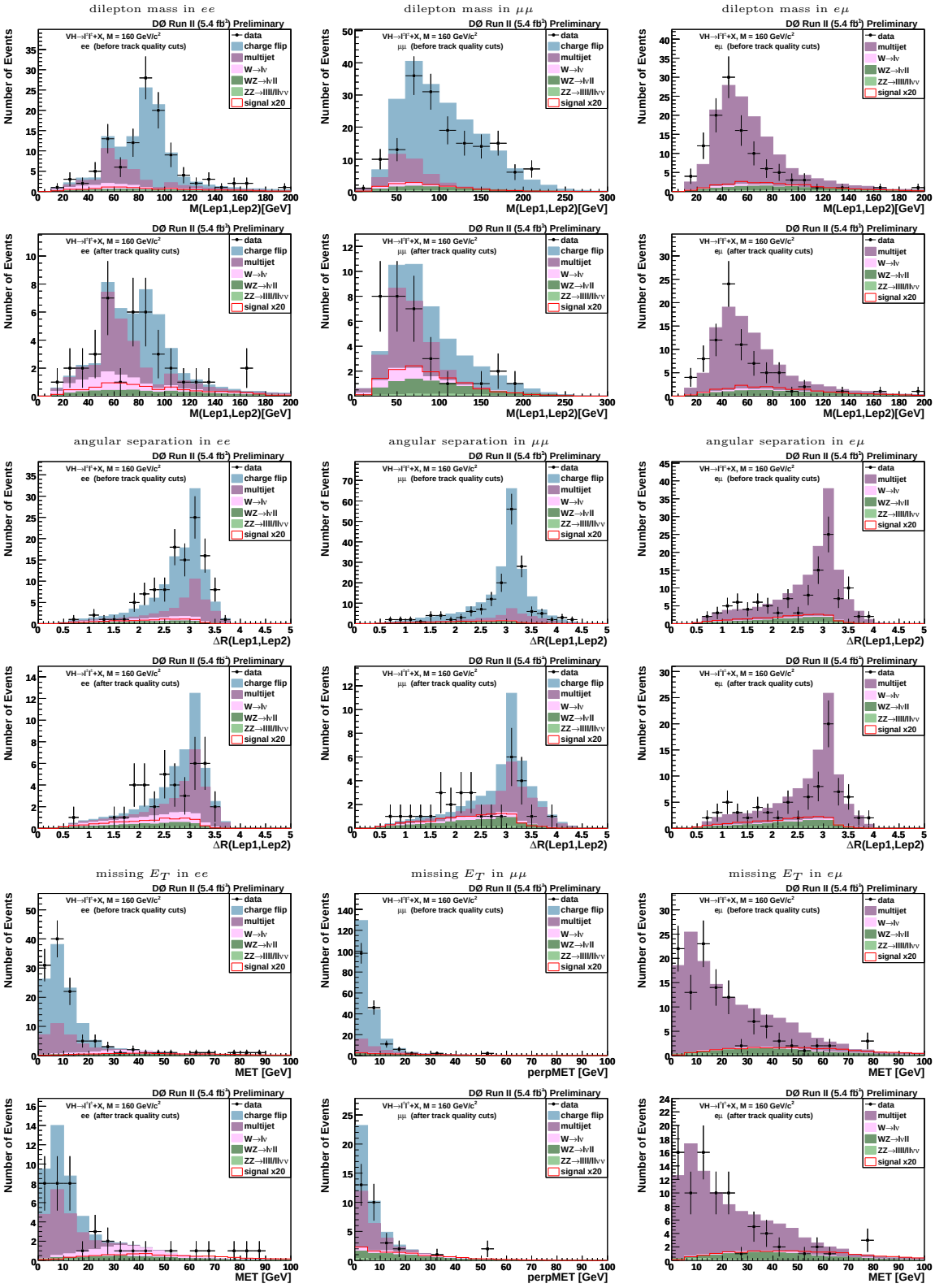

FIG. 1: The distribution of dilepton invariant mass, angular separation between the leptons and the missing transverse energy in the ee (left), $\mu\mu$ (middle), and $e\mu$ (right) channel before the track quality requirements (row 1, 3, 5) and after all the selections (row 2, 4, 6). For $\mu\mu$ channel, the component of the missing E_T perpendicular to one of the muons (details in Section VII) is used.

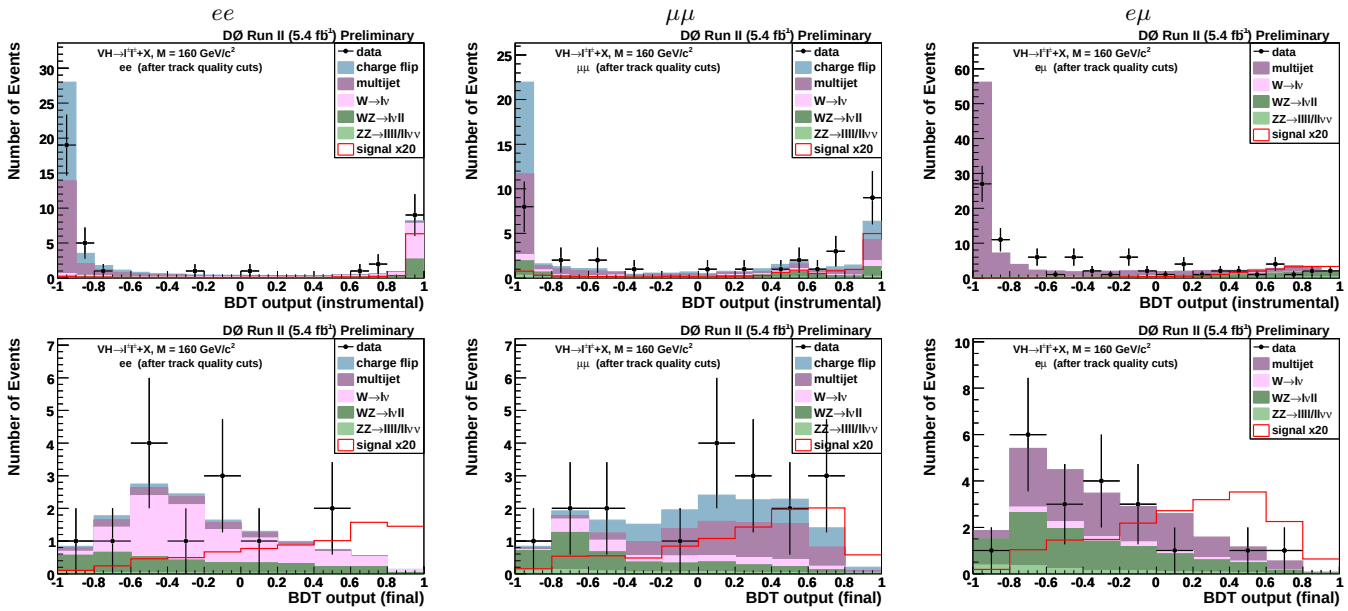

FIG. 2: *The distribution of the BDTG discriminant against instrumental backgrounds (top) and the final discriminant (bottom) which is an effective product of the instrumental and physics BDT outputs after a cut at BDT(instrumental) > 0.0. Data and background predictions corresponding the integrated luminosity of 5.4 fb^{-1} are shown for the assumed Higgs mass of 160 GeV.*

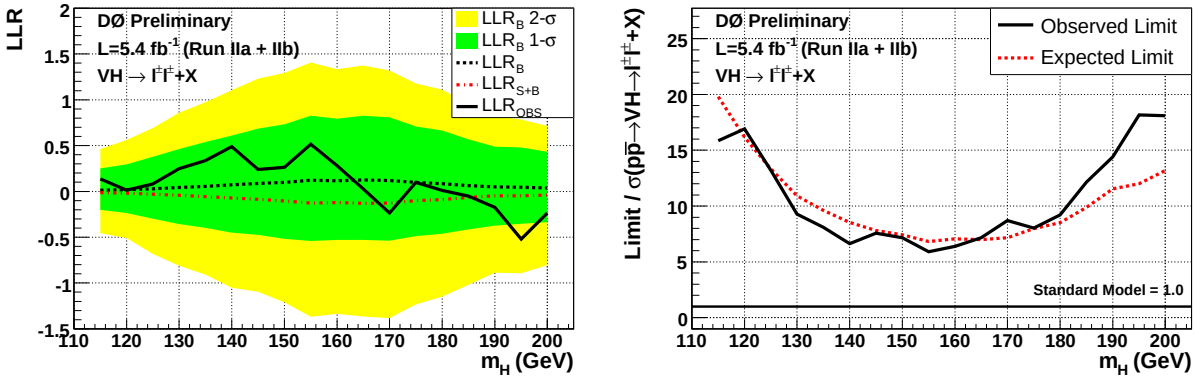

FIG. 3: Right: the logarithmic likelihood ratios (LLR) for the tree channels combined at 5.4 fb^{-1}. Lower dashed line: LLR for the signal + background hypothesis; upper dashed line: LLR for the background-only hypothesis; full line: observed data; green (yellow) bands: 1 (2) standard deviation for background-only LLR. Right: expected and observed upper limits on $\sigma(WH) \times Br(H \to WW^*)$ at the 95% confidence level, as a ratio to the standard model cross section.